1-3 Observations of Aurora and Atmosphere-Plasma Interaction

Optical Interferometry Techniques and Scientific Results for the Dynamics of the Upper Atmosphere in the Alaska Project

ISHII Mamoru, KUBOTA Minoru, MURAYAMA Yasuhiro, Mark CONDE, Roger W. SMITH, OKANO Shoichi, and SAKANOI Kazuyo

We developed Fabry-Perot interferometer named NICT-FPI in Alaska project and have observed in several observatories in domestic and overseas. We deployed the instruments at Poker Flat research range and Eagle observatory, Alaska on 1998 and started the observation of aurora optics for deducing the neutral-ion coupling and vertical winds with active aurora. We can expect the technique to be widely applied in many fields, e.g., laser technology.

Keywords
Fabry-Perot Interferometer, Thermosphere, Joule heating, Ionospheric convection, Vertical wind

1 Outline and principle of observation of the Fabry-Perot interferometer

A detailed description of the principle of the Fabry-Perot interferometer (hereafter "FPI") has been presented in a previous paper[1], so only a brief outline required for understanding the present report will be given here.

The FPI is an instrument that separates out light of a specific wavelength (or frequency) through multiple reflections and interference between two glass plates called etalons. The instrument is used in a wide range of applications, including laser transmissions.

The instrument offers wavelength resolution on the order of picometers. Thus, when a light-emitting body is moving at speed of approximately 10 m/s, the exact speed of motion can be calculated based on the Doppler velocity of the emitted light, measured via remote sensing. Further, if the emitting body is in a thermally vibrating gaseous state, its temperature may be estimated from Doppler broadening.

We have conducted observations of airglow emissions at altitudes of 85～250 km in the terrestrial atmosphere using this instrument, and have developed technologies for estimating wind direction, speed, and air temperature at each altitude level. One of the most widely known airglow phenomena is found in the auroral events seen in the polar regions. Other airglow phenomena may be observed globally—although at much weaker emission intensities—and meteorological observations of the upper atmosphere using FPI are possible even in the middle to lower latitude regions.

The atmosphere up to an altitude of approximately 300 km (including the middle atmosphere at 10～80 km) does not offer favorable conditions for direct stationary observations using balloons or artificial satellites, and so observation of this region relies mainly on remote sensing techniques. The middle and upper atmospheric regions in the polar regions display complex dynamics due to the effects of solar activity—as with the aurora—in addition to the effects of weather/climate conditions near the Earth's surface. The solar energy input from auroras are negligible compared to that from solar radiation, but since the influx of this energy occurs in a limited region, it cannot be ignored when performing atmospheric simulations. Furthermore, variations in atmospheric composition have been recognized to display a strong relation to polar dynamics, and changes in the polar O/N_2 ratio have been attributed to ionospheric storms occurring in the middle to low latitude regions.

2 Outline of the instrument

In the FPI developed for the Alaska Project (referred to below as the "NICT-FPI"), two types of instruments were developed: a scanning FPI and an all-sky FPI. The scanning FPI is a conventional type of instrument that uses mirrors to make observations of a relatively limited area in the selected region of the sky. In contrast, the all-sky FPI performs observation of the entire sky at once using a fish-eye lens. Figure 1 presents a schematic view of the optical system of the NICT-FPI. (See [1]-[3] for instrument details.)

One feature of the NICT-FPI is that it can perform simultaneous observation of two wavelengths using a dichroic mirror. This in turn enables simultaneous measurement of wind velocity and temperature at heights corresponding to the observed airglow emissions.

The main consideration in the development of the NICT-FPI was not in the development of the optical element itself but in the assembly and stability of operating the system as a whole. Special focus was placed on developing technology for remote and automatic system operation—such as temperature management in the etalon, which is sensitive to surrounding temperature conditions; a laser calibration technique for monitoring the etalon-gap drift (compatible with 2-wavelength observation); and a cooling system for the water-cooled photon-counting imager.

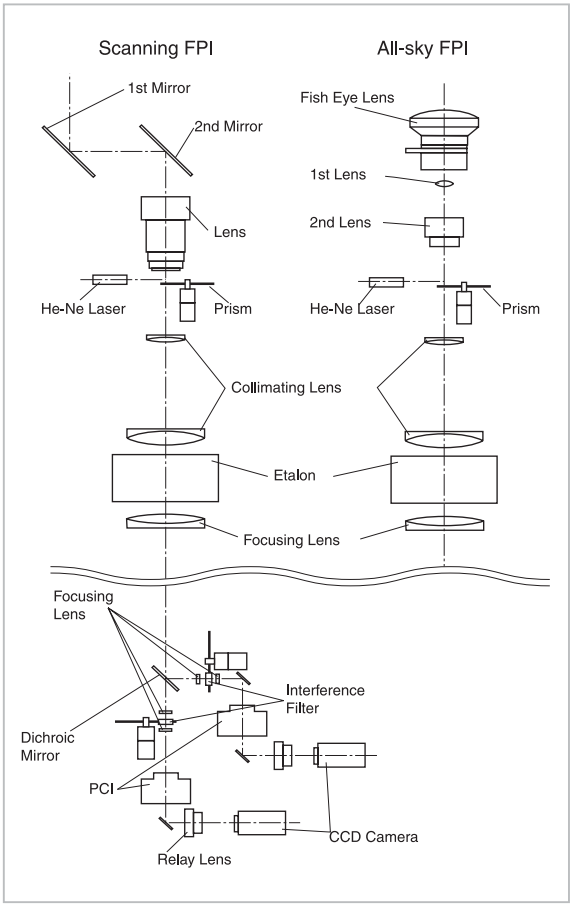

Fig. 1 *Schematic diagram of the optical system of NICT-FPI*

One of the common airglow phenomena observed by the FPI is atomic oxygen emission at wavelengths of 557.7 and 630.0 nm. In recent years, improved detector sensitivity has resulted in the inclusion of weaker OH emissions (at 843.0 nm, for example) in observations. Observations of 557.7-nm emissions are effective for wind velocity and temperature estimations in the lower thermosphere and the mesosphere (peak altitude of approx. 95 km for airglow and approx. 110 km for auroras); and 843.0-nm emissions are effective for both

airglow and auroras (altitude of 86 km, respectively); and 630.0-nm emission observations are effective in the higher ionospheric F layer (peak altitude of approx. 250 km).

3 History of observation

The development of the NICT-FPI began in 1993, and after pilot observations both in Japan and abroad, in 1998 versions of this instrument were installed at the Poker Flats Research Range (scanning FPI) and the Eagle Observatory (all-sky FPI) in Alaska.

Below is a summary of a history of observations of this instrument.

From Nov.-Dec. of 1993, an operational check and successful first-time observation of airglow took place at the Zao observatory, Tohoku University. In 1994, performance was checked against the MU radar at the Shigaraki MU Observatory of Kyoto University by comparing the measurement results obtained from simultaneous observation with the MU radar. Then, in Mar.-Sep. 1996, the NICT-FPI was relocated to the Yamagawa Observatory of the Communications Research Laboratory (currently NICT), to participate in the observation of a rocket launched from the Kagoshima Space Center (Uchinoura) of the Institute of Space and Astronautical Science (currently JAXA) (the SEEK Campaign).

In Jan.-Feb. 1997, simultaneous observations were made with the EISCAT radar at the EISCAT Ramfjordmoen site in Norway along with the first auroral observation by the NICT-FPI, in addition to data collected by both the radar and the NICT-FPI on neutral-ion coupling[4]. In 1998, the instrument was moved back to the Shigaraki MU Observatory of Kyoto University, and simultaneous observations with the MU radar were performed along with pilot operation of the automated observation system before final relocation to Alaska in Sept. 1998.

4 Major observation results

Here we will introduce two major results achieved through observations using NICT-FPI.

Fig.2 *Overview of the Various Observatories (top: EISCAT; middle: Poker Flat Research Range; bottom: Eagle Observatory)*

4.1 Dragged neutral

At altitudes of approximately 100 km in the polar atmosphere, the collision between ions and neutral atmosphere results in the exchange of kinetic momentum. This region also displays a horizontal circulation of ions induced by high-speed plasma from the Sun. The ions comprise approximately 1 % of the atmosphere at an altitude of 250 km, and only 0.01 % at 100 km, but neutral atmosphere has

been known to be dragged along by ion flow when such a flow has been present stably for a certain length of time. Further, when a drastic change in ion flow is induced (such as by inversion of the interplanetary magnetic field), the neutral atmosphere does not seem to react at once; instead, heating occurs through collision with the flow (the so-called "flywheel" effect)[5].

In the past, observations of neutral-ion coupling have been conducted using artificial satellites[6], but such studies could only obtain snapshots of the phenomenon in question. With the NICT-FPI, however, we have conducted simultaneous observation of both the neutral atmosphere and ions from the ground jointly with the SuperDARN radar, and have succeeded in estimating atmospheric motions over time.

Figure 3 presents the velocity vectors of neutral atmosphere and ions measured by simultaneous observation using NICT-FPI and the HF radar of Saskatchewan University and the University of Alaska on Nov. 24, 2000. At 06:43 UT, neutral wind (blue) is present in the westerly direction, while the plasma flow (red) is moving toward the northwest. However, from approximately 07:00 UT, the plasma flow stabilizes and begins to accelerate in the northwest direction. In response, the velocity of the neutral wind also shifts its direction to the northwest, gaining speed. At 08:46 UT, the neutral wind reaches 180 m/s in response to a plasma flow of 300 m/s.

4.2 Thermospheric vertical winds associated with auroral activities

Scientists long believed that no vertical winds exceeding several centimeters per seconds are present in the thermosphere. This belief led to the adoption of the vertical motion observed by the FPI as an indicator of

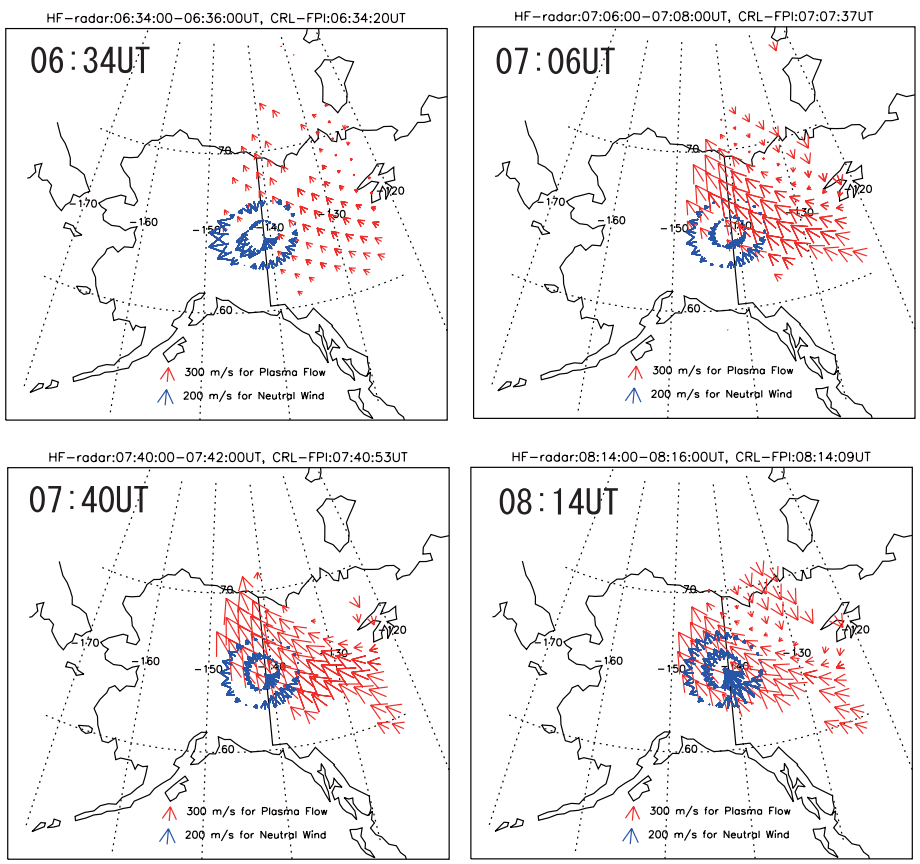

Fig.3 Variations in the ions and neutral atmosphere observed on Nov. 24, 2000

zero wind speed, which was otherwise difficult to obtain. However, in 1984, Rees et al.[7] observed, for the first time, thermospheric vertical winds exceeding 100 m/s in the auroral zone, and this discovery initiated a debate on the possible causes and effects. Since the existence of the vertical wind should affect movement based on kinetic momentum as well as the compositional structure of the atmosphere, we may need to significantly modify our conventional understanding of the thermospheric structure.

At the Halley's Observatory in Antarctica, Crickmore et al.[8] have observed that strong downward winds at approximately 50 m/s are often present when the observatory falls near the equatorial boundary of the auroral oval. Price et al.[9] made observations at 557.7 nm (at an emission altitude of approx. 110 km) and 630.0 nm (approx. 240 km), and concluded that strong upward winds are present at both altitudes near the poleward auroral oval boundary. Furthermore, Innis and Conde[10] performed statistical analysis of the polar vertical winds over a wide area using an instrument known as WATS aboard the DE-2 satellite, which measures wind in the proximity of the satellite. Their results showed that strong vertical winds are present both in the northern and southern hemispheres, especially near the morning side of the polar cap. Their statistical study will no doubt represent a lasting contribution to atmospheric modeling. On the other hand, difficulties remain in discussing individual events, which inhibits the application of these events to general discussions on resolving the mechanism of vertical wind generation. In any case, all of the results obtained by different observation methods have been consistent, and we believe that it is safe to say that the existence of the vertical wind in the polar thermosphere has been established.

Based on these and similar studies, we conducted observation of the thermospheric vertical winds using NICT-FPI at the Poker Flat Research Range in Alaska. Our observations, featuring high temporal resolution (approx. 2 minutes) at 557.7 nm and 630.0 nm over an extended period, allowed for statistical analysis of vertical wind behavior at the two altitude regions of 110 and 240 km. The example presented here reflects observations using the scanning NICT-FPI installed at Poker Flat, Alaska for the period from Oct. 1998 to Feb. 1999. The observations were made at a temporal resolution of 2 minutes in the visible emission range (557.7 and 630.0 nm) for atomic oxygen in the thermosphere. Auroral luminance data in the magnetic N-S direction taken using a meridional scanning photometer of the University of Alaska was used as simultaneous observation data.

Figure 4 presents some of the results of these observations. The horizontal and vertical axes represent the zenith angle from the observation point and the auroral luminance distribution (557.7 nm), respectively. The auroral distribution corresponding to the period when upward or downward winds were observed by the NICT-FPI differs significantly from the average distribution of the whole dataset, and during upward winds the zenithal and poleward luminance seem to drop. In contrast, during downward winds, the poleward luminance increases while the equatorial luminance decreases. This may suggest that different wind systems are present in different regions in the aurora[11].

The disadvantage of vertical wind observation with the FPI is that only an extremely limited area directly above the instrument can be observed. To compensate for this, we have carried out a project of simultaneous observation using two NICT-FPI units located approximately 300 km apart. This was originally part of ground support in rocket observations of thermospheric vertical winds (the HEX campaign), and was the first instance anywhere of simultaneous observation of vertical winds using multiple FPIs. The all-sky FPI installed at Eagle Observatory was specially equipped with a telescopic lens for observing vertical winds during the campaign period of Feb.-Mar. 2003.

Figure 5 is an example of vertical winds observed on Mar. 21, 2003 using emissions at

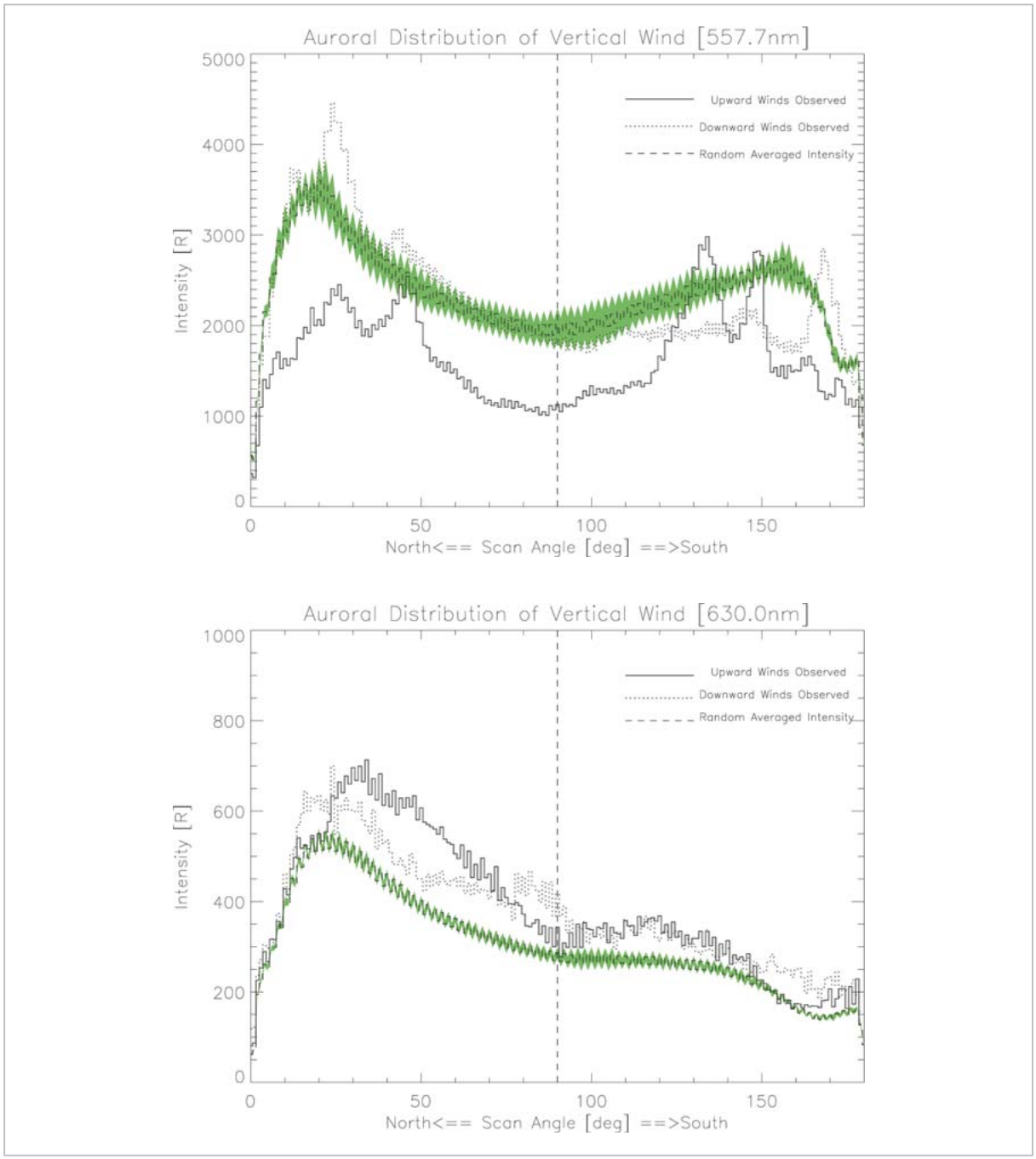

Fig.4 *Distribution of auroral luminosity along the geomagnetic meridian when the upward and downward vertical winds are observed*

solid line: upward wind, break line: downward wind, dotted line: averaged distribution of luminosity during all observation period.

630.0 nm (a) and 557.7 nm (b); results obtained at two observation points (red: Poker Flat; blue: Eagle) are superimposed. Figs. 5 (c) and (e) show the N-S auroral distributions at Poker Flat, and (d) and (f) show the N-S auroral distribution above Eagle Observatory, simulated from the results of the all-sky imager at Poker Flat.

Significant differences are seen in the results for the 630.0-nm emission, while the wind variations seen for the 557.7-nm emission at the two sites closely resemble one another despite the separation of 300 km between them.

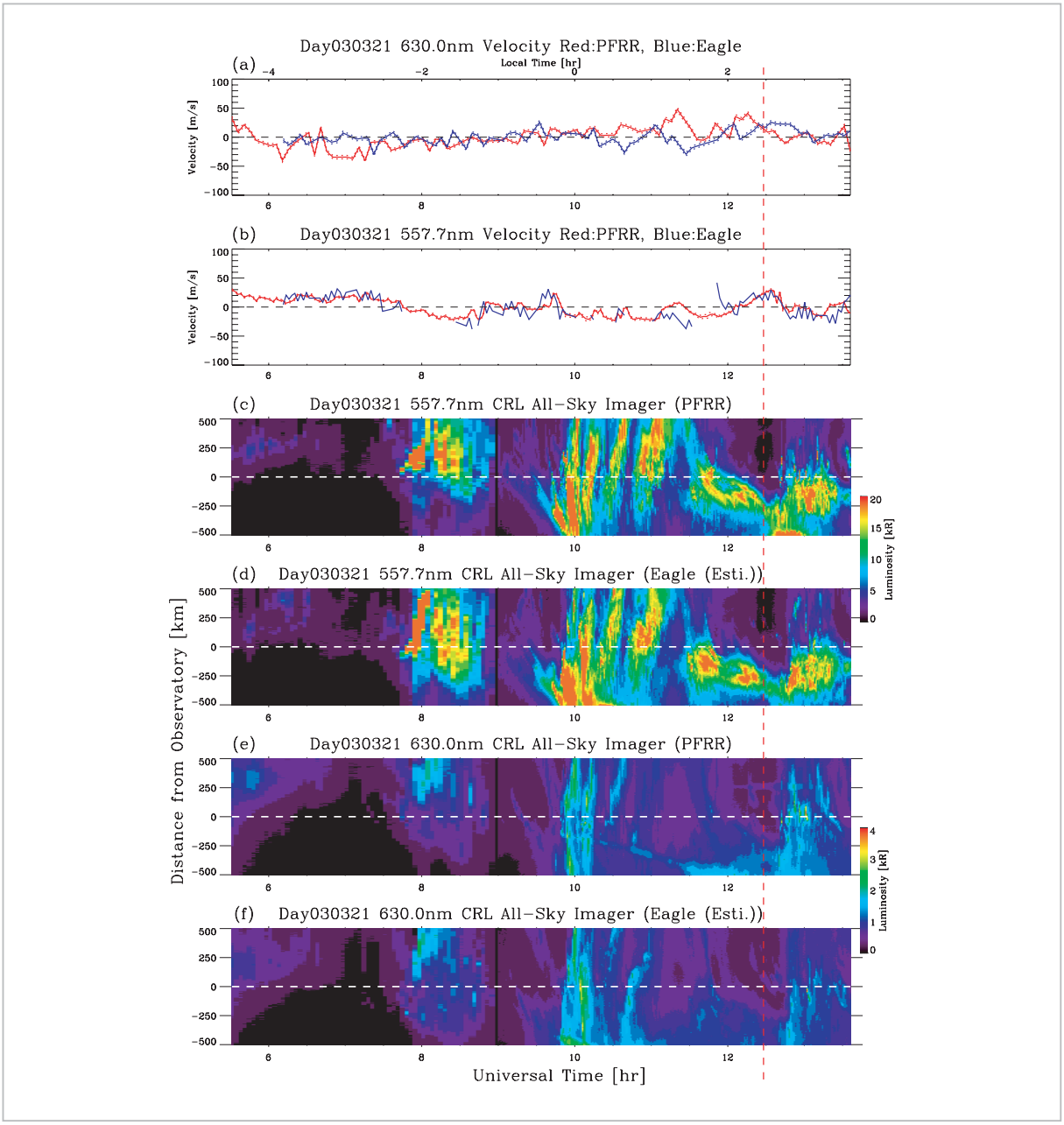

Fig.5 *Examples of observation made on March 21, 2003 of vertical winds*

Table 1 presents the coefficient of correlation for the vertical winds observed at the two sites using two wavelengths (557.7 and 630.0 nm) for each night of the campaign. At 557.7 nm (estimated emission altitude: 110~140 km), vertical winds at PFRR and Eagle displayed a high coefficient of correlation, with six cases in which the value exceeded 0.6.

The high correlation between the wind variations observed at 557.7 nm (estimated emission altitude: 110 km) indicates that the wind system along the auroral arc is uniform, and that the positions of the two stations relative to the aurora are close together. In contrast, from the results corresponding to the 630.0-nm emission (estimated emission altitude: 240 km), it can be seen that in some instances the station positions relative to the aurora were situated differently. Further, if we assume that vertical winds are generated by Joule heating, then the heat source must lie near the 110-km altitude, where the Pederson current dominates. Thus, in regions removed

Table 1 *Coefficients of correlation for wind velocity variations at the two observation sites for each night during the campaign*

Date	Cor. (630.0nm)	Cor. (557.7nm)
Feb. 26	0.147	0.600
Mar. 01	0.345	0.598
Mar. 06	0.069	0.420
Mar. 08	0.121	0.768
Mar. 21	0.198	0.677
Mar. 24	0.336	0.529
Mar. 25	-0.466	-0.01
Mar. 27	0.164	0.104
Mar. 28	0.085	-0.01
Mar. 29	0.100	0.625
Apr. 01	-0.281	0.768
Apr. 02	-0.101	0.233
Apr. 03	-0.119	0.769

from the heat source, effects other than Joule heating will become predominant, which will lead to poor correlation[12].

The examples were observed using emissions at 630.0 nm (a) and 557.7 nm (b) at Poker Flat Research Range (red) and Eagle Observatory (blue). (c) and (e) are N-S auroral distributions observed at Poker Flat for 557.7 and 630.0 nm, respectively, and (d) and (f) are the N-S auroral distributions above Eagle simulated from the results of the all-sky imager at Poker Flat for 557.7 and 630.0 nm, respectively.

5 Conclusions

The Alaska Project ended in FY 2005, but the technologies developed during the project have been handed down to succeeding projects, and the NICT-FPI is expected to play a major role in NICT's 2nd Mid-Term Plan, the "Radio Propagation Project".

The project will focus on the irregular structures of the ionosphere that lead to disruptions in GPS positioning, communications, and broadcasting. The plasma bubble, which is one such irregularity, grows rapidly toward the low-latitude regions after generation in the dusk-side equatorial region and propagates eastwards. Therefore, the plasma bubbles that affect Japan are those generated in Southeast Asia.

While theoretical understanding of the mechanism of plasma bubble generation is rapidly progressing, prediction is still impeded by unknown factors that cause day-to-day variations[13]. One of the parameters that may be required for resolving such unknown factors is the neutral wind in the F layer, and the FPI is expected to become useful in this context. However, the generation of plasma bubbles occurs at dusk, and the observation of neutral winds before and after this time requires airglow observations under conditions of strong solar radiation. It will therefore be necessary to develop a technique for eliminating strong background light. One method that may be effective in resolving this problem involves the use of the tandem etalon Fabry-Perot interferometer[14]. This instrument is currently being developed in the U.S. (and not yet in Japan). If successful, the instrument will no doubt be exceptionally useful in a wide range of optical applications, since it will enable spectral dispersion in the ultra-narrow bands utilized in laser engineering. Accordingly, we believe that this pursuit will represent a valuable basis for further technological innovation.

Acknowledgements

We are grateful to Eiichi Sagawa, Kazumasa Kanda, Yukio Kaneko, Toshiaki Tamura, Fumihiko Kamimura, Dai Sakamoto, Inou Takeuchi, Koichi Yajima, and Katsuko Usui for their cooperation. We also thank all the staff members who have worked in support of the operation of the Zao Observatory of Tohoku University, the Shigaraki MU Observatory of Kyoto University, the Yamagawa Radio Observatory of the CRL, the EISCAT Ramfjordmoen site in Norway, and the Poker Flat Research Range of the University of

Alaska and the Eagle Observatory. We are indebted to Takuji Nakamura, Kazuo Shiokawa, Makoto Taguchi, Takeshi Sakanoi, and all those who have contributed to this work through their valuable advice.

References

1 Ishii, M., S. Okano, E. Sagawa, Y. Murayama, S. Watari, M. Conde, and R. W. Smith, "Development of CRL Fabry-Perot interferometers and observation of the thermosphere", CRL Journal, 49, 2, 173-183, 2002.

2 Ishii, M., S. Okano, E. Sagawa, S. Watari, H. Mori, I. Iwamoto, and Y. Murayama, "Development of Fabry-Perot interferometers for airglow observations", Proc. NIPR. Symp. on Upper Atmos. Phys., 10, 97-108, 1997

3 Ishii, M., S. Okano, E. Sagawa, S. Watari, H. Mori, I. Iwamoto, K. Kanda, F. Kamimura, and D. Sakamoto, "Development of an automatic observation system for Fabry-Perot interferometers", Adv. Polar Upper Atmos. Res., 15, 178-192, 2001.

4 Ishii, M., S. Oyama, S. Nozawa, R. Fujii, E. Sagawa, S. Watari, and H. Shinagawa, "Dynamics of neutral wind in the polar region observed with two Fabry-Perot interferometers", Earth Planet Space, 51, 833-844, 1999.

5 Lyons, L. R., T. L. Killeen, and R. L. Walterscheid, "The neutral wind "flywheel" as a source of quiet-time, polar-cap currents", Geophys. Res. Lett., 101-104, 1985.

6 Killeen, T. L., P. B. Hays, G. R. Carignan, R. A. Heelis, W. B. Hanson, N. W. Spencer, and L. H. Brace, "Ion-neutral coupling in the high latitude F region: Evaluation of ion heating terms from Dynamics Explorer 2", J. Geophys. Res., 89, 7495-7508, 1984.

7 Rees, D., Smith, R. W., Charleton, P. J., McCormac, F. G., Lloyd, N., and Steen, A., "The generation of vertical winds and gravity waves at auroral latitudes — I. Observations of vertical winds", Planet Space Sci., 38, 667-684, 1984.

8 Crickmore, R. I., Dudeney, J. R., and Rodger, A. S., "Vertical thermospheric winds at the equatorward edge of the auroral oval", J. Atmos. Terr. Phys., 53, 485-492, 1991.

9 Price, G. D., Smith, R. W., and Hernandez, G., "Simultaneous measurements of large vertical winds in the upper and lower thermosphere", J. Atmos. Terr. Phys., 57, 631-643, 1995.

10 Innis, J., and Conde, M., "High-latitude thermospheric vertical wind activity derived from Dynamics Explorer 2 WATS observations: Indications of a source region for polar cap gravity waves", J. Geophys. Res., 107, 1172, 10.1029/2001JA009130, 2002.

11 Ishii, M., Conde, M., Smith, R. W., Krynicki, M., Sagawa, E., and Watari, S., "Vertical wind observations with two Fabry-Perot interferometers at Poker Flat, Alaska", J. Geophys. Res., 106, 10,537-10,551, 2001.

12 Ishii, M., M. Kubota, M. Conde, R. W. Smith, and M. Krynicki, "Vertical wind distribution in the polar thermosphere during Horizontal E region Experiment (HEX) campaign", J. Geophys. Res., 109, doi:10.1029/2004JA010657, 2004.

13 Abdu, M. A., "Outstanding problems in the equatorial ionosphere-thermosphere electrodynamics relevant to spread F", J. Atmos. Solar-Terr. Phys., 63, 869-884, 2001.

14 Emmert, J. T., M. L. Faivre, G. Hernandez, M. J. Jarvis, J. W. Meriwether, R. J. Niciejewski, D. P. Sipler, and C. A. Tepley, "Climatologies of nighttime upper thermospheric winds measured by ground-based Fabry-Perot interferometers during geomagnetically quiet conditions: 1. Local time, latitudinal, seasonal, and solar cycle dependence", J. Geophys. Res., 111, doi:10.1029/2006JA011948, 2006.

***ISHII Mamoru**, Dr. Sci.*

Research Manager, Space Environment Group, Applied Electromagnetic Research Center

Dynamics in the Ionosphere and Thermosphere

***KUBOTA Minoru**, Dr. Sci.*

National Institute of Information and Communications Technology

Dynamics in the Ionosphere and Thermosphere

***MURAYAMA Yasuhiro**, Dr. Eng.*

Planning Manager, Strategic Planning Office, Strategic Planning Department

Dynamics in the Thermosphere and Mesosphere

***Mark CONDE**, Dr. Eng.*

Fairbanks, University of Alaska

Dynamics in the Thermosphere and Mesosphere

***Roger W. SMITH**, Dr. Eng.*

Fairbanks, University of Alaska

Dynamics in the Thermosphere and Mesosphere

***OKANO Shoichi**, Dr. Sci.*

Professor, Tohoku University

Dynamics in the Thermosphere and Mesosphere

***SAKANOI Kazuyo**, Dr. Sci.*

Komazawa University

Dynamics in the Thermosphere and Mesosphere